# Nanofilled Polyethersulfone as Matrix for Continuous Glass Fibers Composites: Mechanical Properties and Solvent Resistance

**M. AURILIA**

*IMAST – Technological District on Polymeric and Composite Materials Engineering and Structures, Piazzale Enrico Fermi, Località Granatello 1, 80055 Portici (NA), Italy*

**L. SORRENTINO**

*IMCB-CNR – Institute of Composite and Biomedical Materials, Piazzale Vincenzo Tecchio 80, 80125 Naples, Italy*

**L. SANGUIGNO**

*IMAST – Technological District on Polymeric and Composite Materials Engineering and Structures, Piazzale Enrico Fermi, Località Granatello 1, 80055 Portici (NA), Italy*

**S. IANNACE**

*IMCB-CNR – Institute of Composite and Biomedical Materials, Piazzale Vincenzo Tecchio 80, 80125 Naples, Italy*

**ABSTRACT:**   Polyethersulfone (PES) is high performance thermoplastic polymer; however, its applications are limited by the poor resistance to several classes of solvents. Fumed silica and expanded graphite nanoparticles were used to prepare nanofilled PES by a melt-compounding technique with the view to improve the barrier properties. Solvent uptake at equilibrium and solvents resistance of nanofilled PES compounds were investigated by three different methodologies: (1) weight increase by methylene chloride absorption in a vapor-saturated atmosphere, (2) solvent uptake of acetone at equilibrium, and (3) decay of storage modulus induced by acetone diffusion. The storage modulus decay was measured by means of dynamic mechanical analysis on samples immersed in an acetone bath. The collected data were fitted to an ad hoc model to calculate the diffusion coefficient. The produced nanofilled PES showed a significant improvement in barrier properties and considerable reduction in acetone uptake at equilibrium, in comparison with the neat PES. Nanofilled PES compounds were also used to produce continuous glass fiber composites by the film-stacking manufacturing technique. The composites exhibited, by and large, improvements in flexural and shear strength. Their solvent resistance was evaluated by measuring the variation of mechanical properties after exposure to acetone for 1 and 5 days. These tests showed that the composites produced with the nanocomposite matrix did not exhibit higher solvent resistance than those prepared with neat PES, probably because of the deterioration of the fiber/nanocomposite-matrix interfacial bond in the wet state.   © 2010 Wiley Periodicals, Inc. Adv Polym Techn 29: 146–160, 2010; View this article online at wileyonlinelibrary.com. DOI 10.1002/adv.20187

**KEY WORDS:**   Composite, Nanocomposites, Poly(ether sulfones), Solvent resistance, Thermoplastic, Thermoplastic matrix composites

# Introduction

**P**olyethersulfone (PES) is a transparent amorphous thermoplastic polymer with a very high thermal oxidation resistance. Its most important features include high modulus, mechanical strength, a high glass transition temperature ($T_g$ around 230°C) and a continuous operating temperatures in the region of 180°C, as well as good electrical insulation properties.[1] PES has a heat deflection temperature (HDT) in the region of 200°C, which is significantly higher than that of high performance semicrystalline polymers, such as polyetheretherketone (PEEK with HDT = 160°C) and polyphenylenesulfide (PPS with HDT = 135°C) and can be processed at lower temperatures. Moreover, the processing temperature of PES is not higher than many commodity polymers, such as polycarbonate, polyamide 6.6, and polyethylenetherephthalate.[2]

   PES is used in many fields of engineering application, such as in manufacture of pumps and valves for use in the petrochemical industry, medical devices (mainly because it can be sterilized repeatedly), and in environmental engineering. Another use of PES is as matrix in thermoplastic composites, exhibiting mechanical and thermal properties comparable to those of PEEK matrix composite.[3,4] Carbon fiber reinforced PES manufactured through solution impregnation methods have been found to have a high flexural modulus and strength.[5] The main limitation to application of PES arises from its poor solvent resistance, as it can absorb hydraulic fluids, ketones, and esters and can dissolve in chlorinated hydrocarbons.[2] However, it has been shown that the solvent resistance of many polymers can be improved by the addition of nanofillers. Polymeric nanocomposites based on both layered silicates[6−9] and nanosilica particle[10,11] have been found to exhibit a substantial reduction in solvent uptake with a corresponding improvement in barrier properties relatively to the unfilled polymer. In particular, the reduction in permeability in nanocomposites was attributed to the good dispersion of the nanoparticles, which brings about an increase in the diffusion

path tortuosity. The reduction in solvent uptake at equilibrium in nancomposites, on the other hand, was attributed to the strong interactions between the polymer and the nanofiller and to the good dispersion, which increases the available surface area of the reinforcing phase. Conversely, filler with low interaction with the polymer results in solvent uptake that may even exceed that of the unfilled polymer.[6]

Moreover, polymer nanocomposites have been successfully used as matrix in continuous fibers composites as a means of reducing their moisture absorption and to extend their service temperature,[12,13] as well as to improve their mechanical and functional properties.[9,14,15]

This article presents and discusses the results of a study aimed at improving the resistance of PES to solvents by means of nanoparticles addition and also at the evaluation of nanofilled PES as a matrix in continuous glass fibers composites. Two different kinds of nanofiller were selected to prepare nanofilled PES, namely round-shaped fumed nanosilica particles and expanded graphite platelets, with the purpose to evaluate the effect of their shape factor on both mechanical properties and solvent resistance. In particular, nanosilica particles were selected for their high surface area (BET = 380 $m^2$/g-Aerosil R380 technical data sheet) and hydrophilic surface (likely compatible with –$SO_2$– groups of PES macromolecules). Expanded graphite was also selected for its ability to be dispersed with very high aspect ratio (~1000) and consequently to obtain a very high specific area (BET = 700–1500 $m^2$/g)[16] of the dispersed phase. The nanosilica and graphite particles were not modified or coated with any organic layer to prevent degradative phenomena caused by the high processing temperatures (~320°C).

# Experimental

## MATERIALS

The PES used was Ultrason E3010, supplied by BASF (Ludwigshafen, Germany). The silica nanofiller was Aerosil R380 (mean average primary particle size = 7 nm, specific surface area = 380 $m^2$/g), obtained from Degussa (Darmstadt, Germany). Proprietary expanded graphite particles (platelets width smaller than 65 μm, platelets thickness smaller than 1 μm, coded TG-741) were supplied by GrafTech International (Anmoore, WV).

The glass fiber woven-fabric VR32 type, (330 g/$m^2$, warp/weft 6.5/5.5) produced by Teximpianti (Brugherio-Milano, Italy) was used as reinforcement for the production of continuous fibers composites. Acetone and methylene chloride (MC) were purchased from Sigma-Aldrich (St. Loius, MO).

## PREPARATION OF NANOCOMPOSITE PES MATRIX

The graphite and silica particles were mixed separately with PES in a Haake Rheocord (Karlsruhe, Germany) internal mixer at 320°C (30 rpm, 5 min, excluded feeding time) to obtain different nanocomposite matrices with several filler contents (0.5, 1.0, 2.5 vol%). These matrices are coded as PES+X%Y, where X% represents the filler volume fraction and Y the type of nanoparticles used (R380 for nanosilica and TG-741 for expanded graphite). A hydraulic press (model P300P, from Collin Gmbh, Bersberg, Germany) was used to prepare 500-μm thick films by compression molding the PES nanocomposites.

## PREPARATION OF CONTINUOUS GLASS FIBER COMPOSITES

The nanocomposite PES matrices were used to prepare fiber-reinforced composite by the film-stacking process. Eight layers of glass fiber fabrics were alternatively stacked with nine layers of PES films in a closed mold. The mold was inserted in the hydraulic hot press, and a three-step pressure-temperature profile was applied (3 min at 360°C and 3 bar, 10 min at 360°C and 15 bar, cooling rate at 10°C/min at 15 bar). The average thickness of composite plates was 1.8 mm.

### CALORIMETRIC ANALYSIS

The thermal properties were evaluated with a differential scanning calorimeter (DSC 2920, TA Instruments, New Castle, DE) under $N_2$ purge over the 30–330°C temperature range. The mass of samples was around 9 mg. The heating and cooling scans were always carried out at a rate of 10°C/min. After holding the specimens at 330°C for 5 min to minimize the effects of previous thermal history, the cooling traces were recorded from 330 to 30°C, and then the second heating scan was performed.

### RHEOLOGICAL ANALYSIS

Rheological measurements were carried out with a strain-controlled rotational rheometer (ARES from

TA Instruments) under $N_2$ flow. 0.5 mm thick disks were loaded onto 25 mm parallel plate fixtures. A dynamic strain sweep test at 1 rad/s was performed for each sample to identify the strain range of linear viscoelastic behavior. Then frequency sweep tests were carried out from 1 to 100 rad/s within the linear viscoelastic strain range. All rheological tests were performed at 360°C.

## DYNAMIC MECHANICAL ANALYSIS

Dynamic mechanical tests were carried out by means of a Triton DMA (Tritec 2000 from Triton, Nottinghamshire, UK) in tensile deformation at 1 Hz frequency and heating at rate of 4°C/min from 30° to 300°C. The samples size was 20 mm in length, 5 mm in width, and 0.5 mm thick.

To evaluate the kinetics of solvent absorption by the polymeric matrix, tensile dynamic mechanical analysis (DMA) tests were also performed on samples kept immersed in acetone whose temperature (30°C) was controlled by the chamber tool for liquids of the DMA instrument (equipped with a temperature control system). The measured storage modulus decay, caused by solvent diffusion, was predicted by a model through a data-fitting procedure, and the diffusion coefficient of acetone in the PES matrices was obtained through fitting parameters (see later).

## SOLVENT UPTAKE TESTS

Two types of solvent uptake tests were carried out to study the effects of the dispersed nanoparticles on both barrier properties and solvent absorption up to equilibrium conditions. In the first method, specimens with 25 mm diameter and 0.5 mm thickness were exposed to MC vapor in a closed chamber at room temperature, in compliance with the standard ASTM D543-95. The percentage gain per unit weight of the along a fixed timeframe was recorded by weighing samples removed from the chamber at regular intervals. The solvent uptake characteristics were established as the mean of three samples measurements.

In the second test method, each specimen (diameter = 25 mm, thickness = 0.5 mm) was fully submerged in acetone in a closed chamber at 30°C. The specimens were extracted from the chamber at regular time intervals, rapidly wiped to remove liquid acetone from the surface and then weighed until a plateau was reached, which was taken as the solvent uptake value at equilibrium. For this test, acetone was used as solvent since MC completely dissolves PES.

## MICROSCOPIC ANALYSIS

### Optical Microscopy Analysis

Optical analysis in reflection mode was carried out by using a microscope (BX51 from Olympus, Tokyo, Japan) to investigate the extent of fiber impregnation in the composite and the distribution of particles dispersed in the composite matrices. Glass fiber composite samples were prepared by polishing the observation surfaces with wet sandpaper and then with a very fine polishing paste.

### SEM–TEM

Scanning electron microscopy (SEM) analysis was performed on cryogenic fractured surfaces of nanofilled matrices and flexural test fracture surfaces of continuous fibers composites with a Leica S440 (Leica Microsystems, Wetzlar, Germany). All sample surfaces were coated with gold layer before the observations to render conductive the specimen surface.

Transmission electron microscopy (TEM) was carried out with a Philips EM 208 (Eindhoven, The Netherlands) at an acceleration voltage of 100 kV. The specimens for TEM analysis were prepared by microtoming 70-nm thick films from the PES matrices with a LKB ultramicrotome.

The nanosilica dispersion in the PES was examined by SEM and TEM. The expanded graphite particles exhibited electron density very close to that of PES macromolecules and, therefore, the contrast of TEM images was inadequate to identify these particles and to study the particles distributions.

## DENSITY AND FIBER VOLUME FRACTION

The density of the composites was measured by weighing samples in air and water according to ASTM D792-00. Five samples for each composite plate were measured, and the volume fraction of glass fibers was calculated from the density of the components.

## MECHANICAL TESTS

### Flexural Tests

Mechanical flexural tests were carried out at room temperature using an Instron 4204 (USA) universal testing machine on samples cut from composites panels, according to ASTM D790. Samples were 12.5 mm wide, 1.8 mm thick (the actual thickness was

used to calculate the stress values), while the span in the bending test was 36 mm, and the loading point for the test was in the center. Five specimens from each composite panel were tested; subsequently, the average values and standard deviation were calculated from the measured data. To evaluate the effects of solvent on the mechanical properties of composites, flexural tests were also performed on samples immersed in acetone at 30°C. These tests were made in compliance with ASTM C581-03; the selected immersion time intervals in acetone were 1 and 5 days, respectively.

### Short-Beam Shear Tests

Short-beam shear tests were carried out to determine the apparent shear strength of continuous fibers composites, according to ASTM D2344. Five specimens from each composite plate were cut (20 mm length, 1.8 mm thickness, and 10 mm wide). The support span was 10 mm (the actual thickness was used for stress calculation). The average values and the standard deviations of experimental determinations were calculated.

# Results and Discussion

## THERMAL AND DYNAMIC MECHANICAL ANALYSIS

In Table I, the glass transition temperature of the produced nanocomposites, measured from the second DSC scan, is reported. All the samples presented a negligible increase in $T_g$ over that of the base PES. The highest $T_g$ was 230.5°C for sample PES+0.5%TG-741, which is less than 1°C higher than the $T_g$ of neat PES. Indeed, the effect of the presence of nanoparticles on the $T_g$ of the nanocomposites was negligible for all samples, which indicates that the interactions at nanoparticle/polymer interface are rather weak.[17,18]

The results from DMA tests are illustrated in Fig. 1. PES samples containing expanded graphite presented an increase in storage modulus with the filler content over the entire temperature range (30–250°C). The sample PES+0.5%R380 showed an increase in storage modulus, whereas PES+1.0%R380 and PES+2.5%R380 exhibited a reduction in storage modulus relatively to neat PES sample. The loss tangent peaks of PES matrices filled with both nanosilica and expanded graphite shifted toward higher temperatures and their values decreased for all particles content (Table I).

To quantify the reinforcing effect of the nanoparticles, the storage modulus ratio (PES nanocomposite modulus/neat PES modulus) were calculated from DMA data at 40°C (Fig. 2). Sample PES+0.5%R380 showed a 4% modulus increase. The modulus of the samples PES+1.0%R380 and PES2.5%R380 was smaller than that of neat PES. Similar reduction in modulus with the filler content has also been reported by other authors[19,20] in polymers filled with either alumina or nanosilica. This behavior was correlated to aggregation of silica nanoparticles. At higher filler content, the probability of agglomerates formation during melt mixing increases and, therefore, the reinforcing efficiency of the particles is reduced,[21] as it is the case for samples PES+1.0R380 and PES+2.5%R380 (Fig. 2). SEM examinations have confirmed the occurrence of an

**TABLE I** ￭
**Summary of Data for PES Nanocomposites**

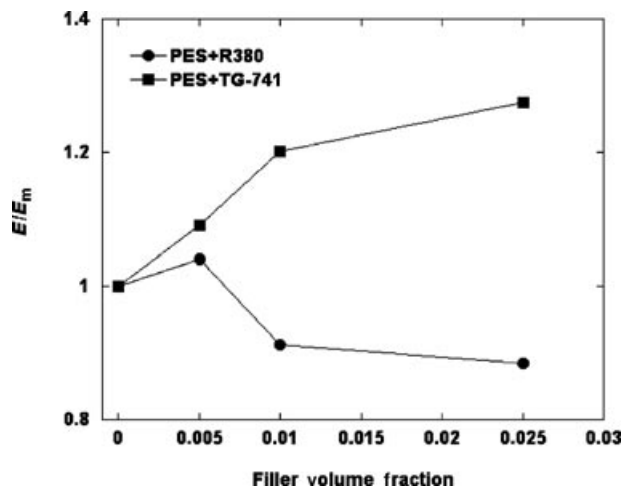| SAMPLES | $T_g$ – DSC (°C) | $T_g$ – DMA Loss Tangent Peak (°C) | Loss Tangent Peak Value | Aspect Ratio DMA | Aspect Ratio Diffusion Coefficient | Acetone Uptake at Equilibrium (wt%) |
|---|---|---|---|---|---|---|
| Neat PES | 229.6 | 233.6 | 2.44 | // | // | 40.0 ± 0.8 |
| PES+0.5% R380 | 230.3 | 238.0 | 2.19 | // | // | 35.8 ± 1.1 |
| PES+1.0% R380 | 230.1 | 237.8 | 2.32 | // | // | 36.6 ± 0.6 |
| PES+2.5% R380 | 230.4 | 238.5 | 1.94 | // | // | 38.4 ± 0.9 |
| PES+0.5% TG-741 | 230.5 | 235.9 | 2.42 | 18 | 132 | 33.2 ± 1.4 |
| PES+1.0% TG-741 | 229.9 | 235.8 | 2.41 | 20 | 63 | 32.0 ± 0.5 |
| PES+2.5% TG-741 | 230.3 | 236.2 | 2.26 | 9.3 | – | 32.0 ± 0.7 |

Glass transition temperatures of nanofilled PES samples measured by DSC run and DMA analysis. Loss tangent peak temperature were measured by DMA. Aspect ratio of graphite particles calculated from both Halpin–Tsai (DMA) and Lape–Cussler models (diffusion coefficient). Acetone uptake at equilibrium was measured at 30°C. //: not evaluated.
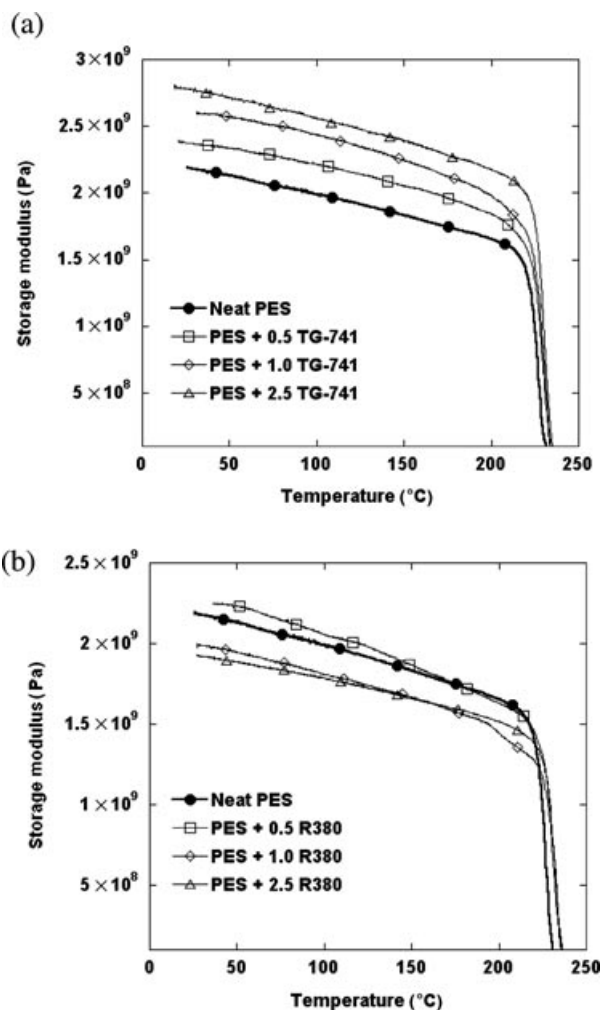
**FIGURE 1.** Temperature scan DMA test on PES samples containing (a) expanded graphite and (b) nanosilica particles.



**FIGURE 2.** Modulus enhancement ratio as a function PES filler content.

system of equations was used:

$$\frac{E}{E_m} = \frac{1 + \zeta\eta\phi_f}{1 - \eta\phi_f} \tag{1}$$
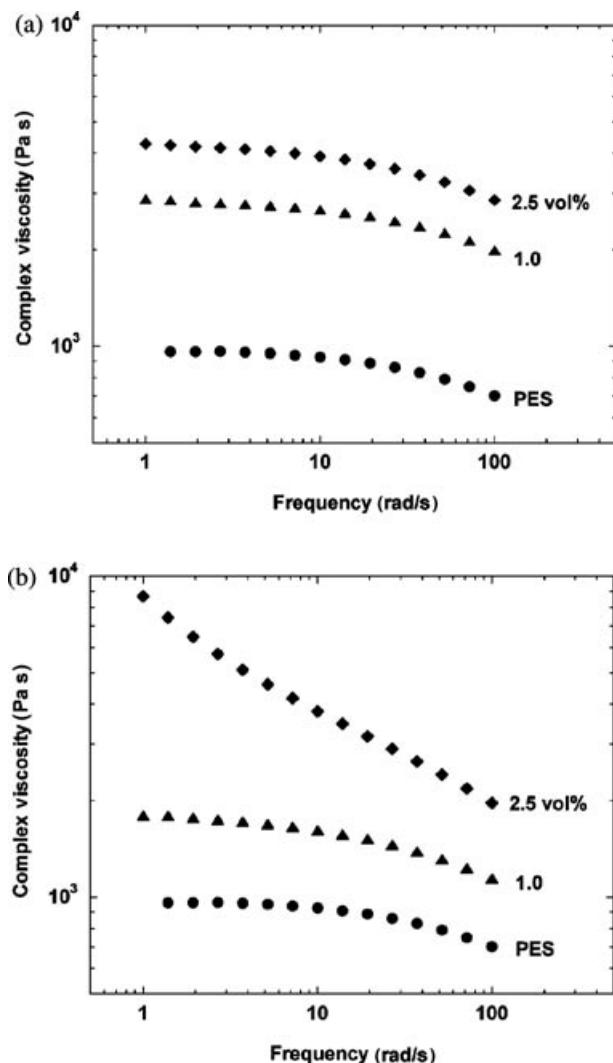
$$\eta = \frac{E_f/E_m - 1}{E_f/E_m + \zeta} \tag{2}$$

$$E_{\text{ran-}3D} = 0.49E_{||} + 0.51E_{\perp} \tag{3}$$

where $E$, $E_f$ (1 TPa),[16,28] $E_m$ (2.2 GPa), and $E_{\text{ran-}3D}$ are, respectively, the Young's modulus of the composite, of the filler (for platelets, it represents the in-plane modulus), of the matrix and that of the nanocomposite containing the randomly dispersed platelets, $\zeta$ is a shape parameter dependent upon filler geometry and loading direction, $\varphi_f$ is the filler volume fraction.[22]

The calculated aspect ratio of graphite platelets ranges from 9.3 to 20 (Table I). A dependence of exfoliation degree on filler content has been previously estimated in organo-modified montmorillonite systems.[29] Other authors[12] showed a decrease in the silicate platelets aspect ratio with increasing filler content, calculated with the H–T model.
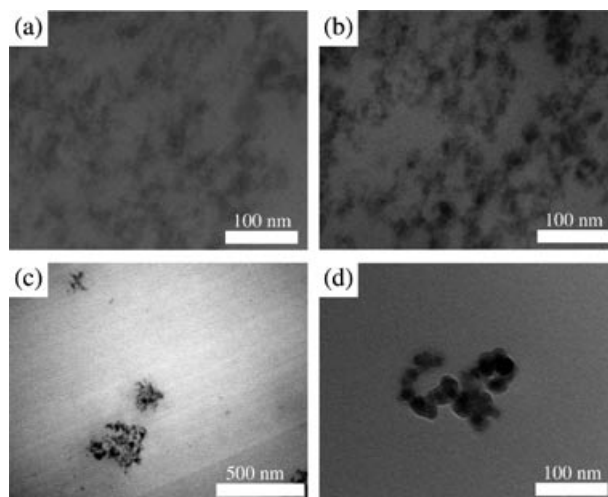
## RHEOLOGICAL ANALYSIS

The variation of the complex viscosity with the frequency of the nanocomposites produced is shown in Fig. 3. This indicates that the complex viscosity of PES containing expanded graphite increases appreciably over that of neat PES. The viscosity values of the samples PES+0.5%TG-741 and

increasingly more pronounced agglomeration with increasing the amount of nanosilica in the PES matrix (see later).

Expanded graphite particles have, generally, shown a higher reinforcing efficiency than silica nanoparticles (Fig. 2). This behavior is in agreement with the results presented by other authors on the reinforcing efficiency of platelets nanoparticles[16,22,23] relative to spherical shapes.[19,23–26] A mean aspect ratio of graphite platelets, which gives a measure of the extent of graphite exfoliation, at each concentration was calculated solving a nonlinear equations system based on the Halpin–Tsai (H–T) self-consistent micromechanical model.[9,12,15,22,27] The following

**FIGURE 3.** Complex viscosity measured by dynamic frequency sweep tests of (a) PES+TG741 and (b) PES+R380 composites melt at 360°C.



**FIGURE 4.** TEM image of sample PES+0.5%R380.

PES+1.0%TG-741 were quite similar in the investigated frequency range, whereas the viscosity of sample PES+2.5%TG-741 was higher (Fig. 3a). The viscosity of samples PES+0.5%R380 and PES+1.0%R380 exhibited a similar increase (Fig. 3b). The viscosity of sample PES+2.5%R380 was the highest (also with respect to PES+TG-741 samples), exhibiting very pronounced nonterminal behavior, that is to say that the complex viscosity does not tend a constant value at low frequency, suggesting that there are fairly strong interactions between silica particles and PES macromolecules.[16]

The viscosity variations of the studied systems exert a considerable influence on the manufacture process and mechanical properties of continuous fiber composites produced by the film-stacking method, since the impregnation process of the fibers is dominated by the viscosity of the wetting matrix.

## SEM AND TEM OF NANOCOMPOSITE MATRICES

The TEM images shown in Fig. 4 permit to distinguish different aspects of the morphology of sample PES+0.5%R380. These represent (1) silica nanoparticles well dispersed in PES matrix (Fig. 4a), (2) zones characterized by well-dispersed nanoparticles and agglomerates (Figs. 4b and 4c), and (3) worm-like silica agglomerates (Fig. 5d).[17] In the first two cases, both particles and clusters are smaller than 100 nm, whereas the worm-like agglomerates are characterized by the cross section made up of few silica nanoparticles. They are smaller than 50 nm in thickness, even though the diameter of the spheroid including the worm-like agglomerates is longer than 100 nm.

The SEM examinations on cryogenic fractured surfaces of silica-based nanocomposites have revealed the presence of clusters in increasing number and size with increasing filler content (Fig. 5). The dimension of the agglomerates never exceeds 600 nm.

SEM images of cryogenic-fractured surfaces of PES samples containing expanded graphite showed the presence of platelets of different dimensions (Fig. 6a). Graphite platelets, about 30 nm thick partially embedded in PES matrix, were detected at
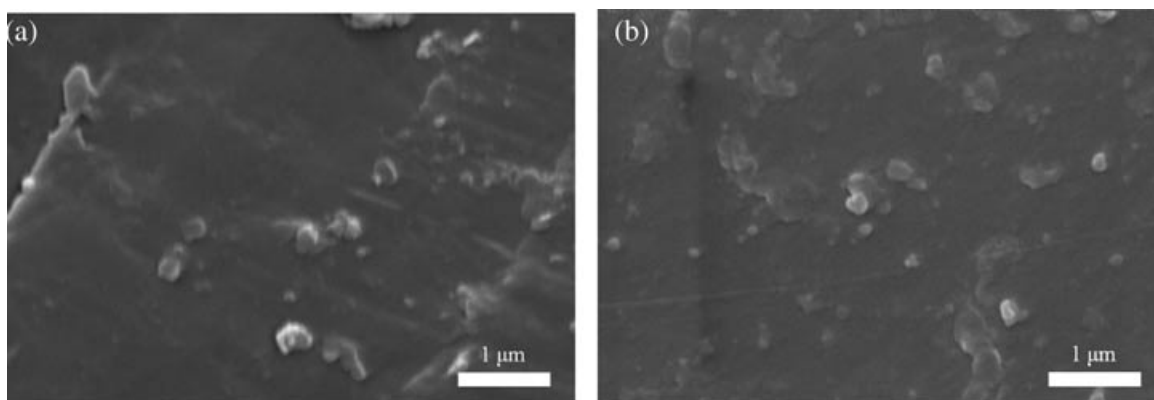
**FIGURE 5.** SEM images of cryogenically fractured PES+0.5%R380 (a) and PES+2.5%R380 (b).
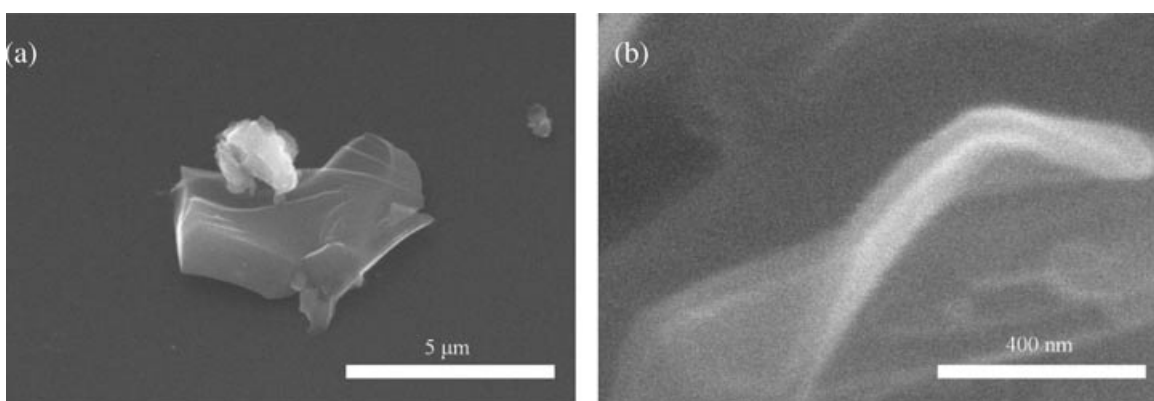


**FIGURE 6.** SEM images of cryogenically fractured PES+0.5%TG741 (a) and PES+2.5%TG741 (b).
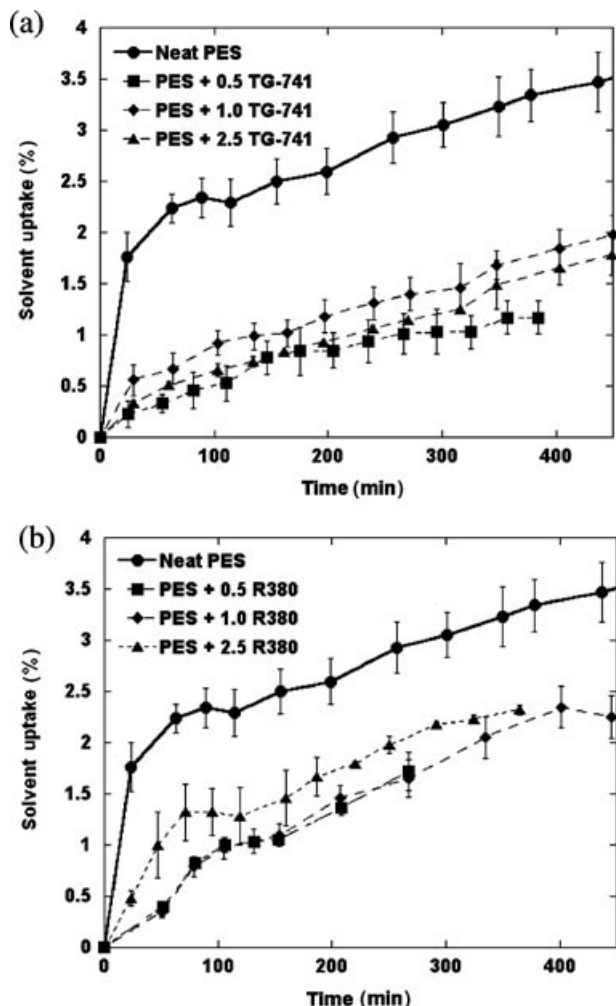
higher magnifications (Fig. 6b). PES+TG-741 samples also displayed an increasing number and different sizes of platelets with increasing filler content. The SEM and TEM investigations have indicated a good dispersion of nanoparticles at nanoscale level for both silica and graphite, as well as the occurrence of agglomerates (note that TEM analyses were not carried out on graphite-based PES matrices). The size of nanosilica agglomerates ranged from 100 to 500 nm, and the width of some graphite nanoparticles was greater than 10 μm. These results are in good agreement with the predictions for fillers dispersion from DMA and rheological tests.

## SOLVENT UPTAKE

The effect of nanoparticles on barrier properties toward MC was investigated at room temperature. All samples containing nanosilica absorbed less solvent than pure PES (Fig. 7b). In the first 60 min, the solvent uptake of the samples filled with nanosilica

was in the region of 0.4–1.1%, whereas the neat PES sample absorbed 2% MC. After 450 min, the MC uptake of neat PES increased to 3.5% whereas that of PES+R380 samples was less than 2%. The barrier effect of graphite particles was even more prominent (Fig. 7a). After 60 min of exposure to solvent, the uptake of PES+TG741 samples was in the region of 0.3–0.7% and after 450 min the highest weight increment registered was 1.75% for sample PES+1.0%TG741. In both nanocomposites systems (filled either with nanosilica or expanded graphite), the highest barrier to the solvent was detected in samples with the lower filler content. This dependence of barrier properties on the filler content, in particular their decrease in nanocomposite with higher filler content, has already been reported by Jana and Jain,[10] who have attributed this effect to the presence of trapped air bubbles around large particle agglomerates of nanosilica, resulting from poor dispersion. A particularly large decrease in solvent absorption was detected in graphite-based nanocomposite due to the
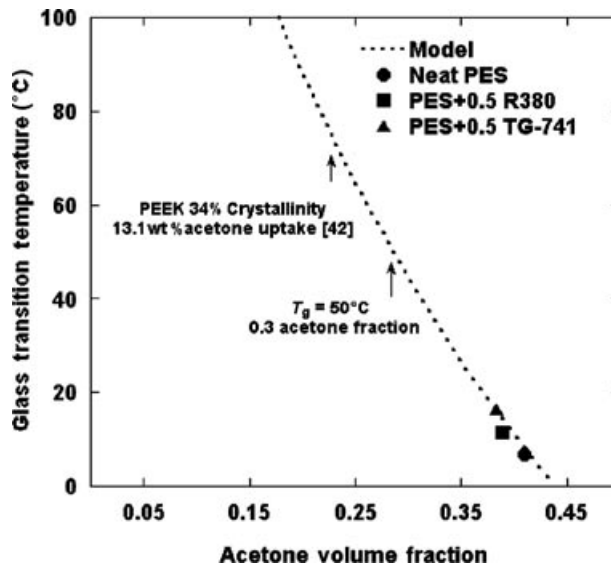
**FIGURE 7.** Uptake of methylene chloride by nanocomposites PES+TG741 (a) and PES+R380 (b).



**FIGURE 8.** Glass transition decrease in PES samples and PEEK as a function of acetone content.

high aspect ratio of graphite platelets. These results are in agreement with other related works.[7,30,31]

Acetone was selected as solvent to investigate the effect of nanoparticles on the amount of solvent absorbed at equilibrium because MC was found to dissolve the samples even in the vapor state. The values for acetone uptake at equilibrium are reported in Table I. These show that all nanocomposite samples absorbed less acetone than neat PES (40.0 wt%). In any case, the graphite-based samples showed a lower solvent uptake compared to silica nanocomposites.

To measure the decrease in $T_g$ resulting from acetone absorption, DSC experiments were carried out at the heating rate of 20°C/min on samples that had reached the sorption plateau by quickly inserting the

samples in a hermetic pan. In Fig. 8, the measured $T_g$ values of the samples neat PES, PES+0.5%R380, and PES+0.5%TG-741 are reported as a function of acetone uptake at equilibrium. The experimental data were compared with a model derived from free volume variation[32] described by the following equation:

$$T_g - T_g' = \frac{\alpha_s(T_g' - T_s)v_s}{\alpha_f(1 - v_s)} \qquad (4)$$

where $T_g$ is the glass transition temperature of the polymer, $T_g'$ is the glass transition of the polymer containing the solvent at the volume fraction $v_s$, $T_s$ is the glass transition of the plasticizer, $\alpha_f$ and $\alpha_s$ are the expansion coefficients of the polymer free volume and solvent, respectively. The values used to predict the $T_g$ variation of PES are reported in Table II.

The plots in Fig. 8 show that the experimental data are in a good agreement with the trend predicted by

**TABLE II**
**Data Used in Eq. (4)**

| $T_g$ PES (°C) | $T_s$ Acetone (Melting Temperature) (°C) | $\alpha_f$ (1/°K) | $\alpha_s$ (1/°K) |
|---|---|---|---|
| 230 | −95 | $4.8 \times 10^{-4}$ | $14.9 \times 10^{-4}$ |

Eq. (4). It is worth pointing out that a 7 wt% reduction in solvent uptake (as for the case of graphite-based nanocomposites) resulted in a 10°C higher $T_g$ with respect to neat PES. This is remarkable in so far as some crystalline aromatic thermoplastic polymers, such as PEEK (34% crystallinity) can absorb larger amounts of acetone (i.e., 13.1 wt% at 35°C). As the solvent would reside in the amorphous phase, it can be predicted that this amount of solvent would result in a 70°C decrease in $T_g$.[33] The calculated $T_g$ values for PEEK have also been inserted in Fig. 8.

It is possible that solvent uptake in PES could be further reduced with (a) finer dispersion of nanoparticles at nanoscale level and (b) improving polymer/nanoparticles bondings.[6,34]

## DMA TESTS ON SAMPLES IMMERSED IN ACETONE

Combining the solution of two-dimensional Fickian diffusion[35,36] in a rectangular cross-section solid with an empirical power law equation, it was possible to fit the experimental data from time scan DMA tests on samples immersed in acetone. This power law equation describes the modulus decay of a solid as a function of solvent content, from which can be obtained the diffusion coefficients. The equation representing the two-dimensional diffusion solution is

$$C(x, y, t)/C_\infty = 1 - \frac{16}{\pi^2} \sum_{m=0}^{\infty} \sum_{n=0}^{\infty} \left( \frac{(-1)^{n+m}}{(2n+1)(2m+1)} \right.$$

$$\times \exp\left( -\frac{D\pi^2 t}{4} \left( \frac{(2n+1)^2}{l^2} + \frac{(2m+1)^2}{r^2} \right) \right)$$

$$\left. \times \cos\left( \frac{(2n+1)\pi x}{2l} \right) \cos\left( \frac{(2m+1)\pi y}{2r} \right) \right) \quad (5)$$

where $C_\infty$ is the constant solvent concentration at the surface, $2l$ and $2r$ are width and thickness of the samples, and $D$ is the diffusion coefficient. The power law equation describing the decrease in modulus with increasing solvent content is

$$E(C) = E_0 \left( 1 - \frac{C}{S} \right)^k \quad (6)$$

where $E_0$ is the modulus of dry matrix, $C$ is the solvent volume fraction in the matrix, $S$ is the solvent content at which the polymer $T_g$ coincides with testing temperature (evaluated from Eq. (4)), and the exponent $k$ defines the nonlinear dependence of the matrix modulus decay upon solvent content.

**TABLE III** ▪
**Fitting Parameters of Eq. (7)**

| Samples | Diffusion Coefficient (cm²/s) | Exponent k | Storage Modulus of Dry Samples $E_0$ (Pa) |
|---|---|---|---|
| Neat PES | 1.19E–07 | 1.06 | 2.47E+09 |
| PES+0.5% R380 | 8.20E–08 | 0.71 | 2.79E+09 |
| PES+1.0% R380 | 9.99E–08 | 0.86 | 2.69E+09 |
| PES+2.5% R380 | 1.98E–07 | 3.00 | 2.40E+09 |
| PES+0.5% TG-741 | 8.16E–08 | 0.90 | 2.66E+09 |
| PES+1.0% TG-741 | 8.19E–08 | 0.93 | 2.85E+09 |

Combining Eqs. (5) and (6) in a surface integral (the concentration is function of the coordinates within cross section of the specimen), the modulus decay as time function $E(t)$ is calculated from

$$E(t) = \int_0^{2l} \int_0^{2r} \frac{E(C(x, y, t))}{4lr} \, dx \, dy \quad (7)$$

where the modulus is the sum of the contributions of different matrix modulus at different solvent concentrations, scaled by their volume fraction. The experimental data were fitted to Eq. (7) by means of an iterative program developed with Matlab software (see Table III). The theoretical model is in good agreement with the experimental data. The proposed model, however, does not take into account plasticization and constrain effects; therefore, it is unable to predict the modulus enhancement occurring over the first minutes of the test. For this reason, $E_0$ was considered a fitting parameter.

The results of the DMA test in acetone of neat PES and only nanocomposites containing 0.5 vol% of nanofillers are shown for better clarity in Fig. 9.

The observation that the diffusion coefficient of nanocomposites decreased nearly by one order of magnitude with respect to neat PES confirms the remarkable improvement in barrier characteristics to toward MC vapor. The smallest diffusivity values were obtained for samples PES+0.5%R380 and PES+0.5%TG-741. The diffusivity of sample PES+2.5%R380 increased relative to neat PES, whereas in sample PES+2.5%TG-741 cracking occurred upon immersion in the solvent and, therefore, it was not possible to perform the tests. The exponent $k$ is an estimation of the resistance of the elastic properties to the solvent, that is the extent by which the matrix storage modulus decreases as
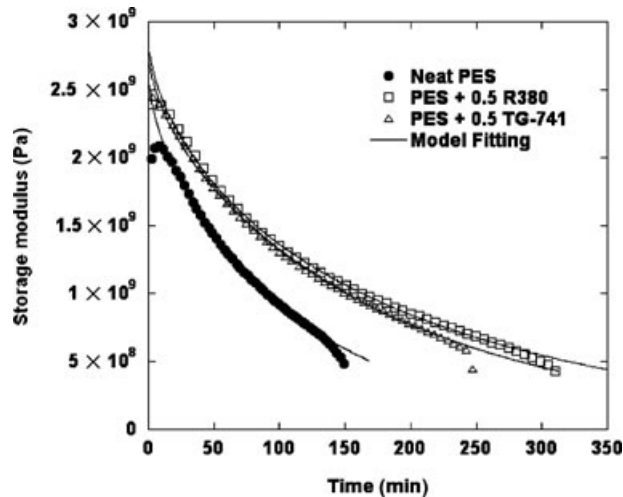
**FIGURE 9.** Time scan DMA tests carried out on samples immersed in acetone at 30°C.

a result of solvent diffusion. This value decrease for all nanofilled samples, except PES+2.5%380, suggests that nanoparticles exhibit a reinforcement effect on the matrix in the presence of acetone. The Lape–Cussler (L–C) model[31] was used to describe the diffusivity decrease of graphite-based nanocomposite and also to obtain the aspect ratio of nanoparticles dispersed in the matrix (Table I). In this model, the filler is assumed to be a ribbon of infinite length (width $= w$, thickness $= t$, aspect ratio $w/t$), dispersed in a random array. For the calculation of the dispersed particles' aspect ratios, the ratio between neat polymer and filled polymer permeability coefficients was approximated with the ratio of diffusion coefficients. The aspect ratios calculated with the L–C model presented a trend with the filler

content similar to that shown by aspect ratios calculated using the H–T equation, since they decreased as the filler content increased. But the aspect ratio calculated with the L–C model for samples PES+0.5%TG-741 and PES+1.0%TG-741 is higher than those calculated with the H–T model. The different values could result from the approximations of Eqs. (5) and (6) or from the geometrical assumptions of the L–C model. Furthermore, it is possible that the efficiency of graphite platelets for mechanical reinforcement is lower than their capacity in providing barrier to solvent diffusion. However, both models were able to estimate a decrease in graphite platelets aspect ratio with increasing filler content, in agreement with observations from SEM examinations showing an increase in graphite platelets dimensions at higher contents. Note that models able to correlate spherical particles dispersion in polymeric matrix to the diffusion coefficient reduction were not found in the literature, hence estimation of dispersed nanosilica particles from diffusion coefficient variation was not obtained.

## MICROSCOPY ANALYSIS OF CONTINUOUS GLASS FIBER COMPOSITES

Optical images of polished surfaces of composite samples have provided useful information on extent of fibers impregnation. For PES filled with graphite, it was also possible to analyze the distribution of visible graphite particles within the composite. Most samples showed very good fiber impregnation and no voids were detected. The neat PES matrix composite (Fig. 10a) showed uniform fibers distribution and good fiber wetting, whereas the composites prepared with the matrices PES+1.0%R380 and PES+2.5%R380 presented
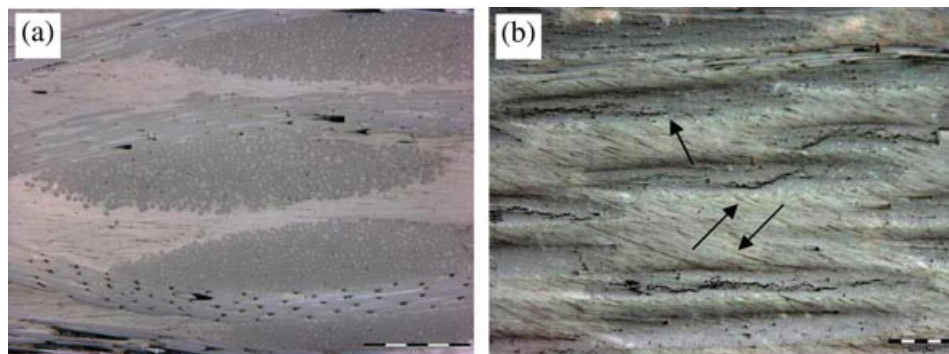


**FIGURE 10.** Optical images of (a) neat PES and (b) PES+1.0%R380 matrices glass fiber composites (the arrows indicate impregnation defects).
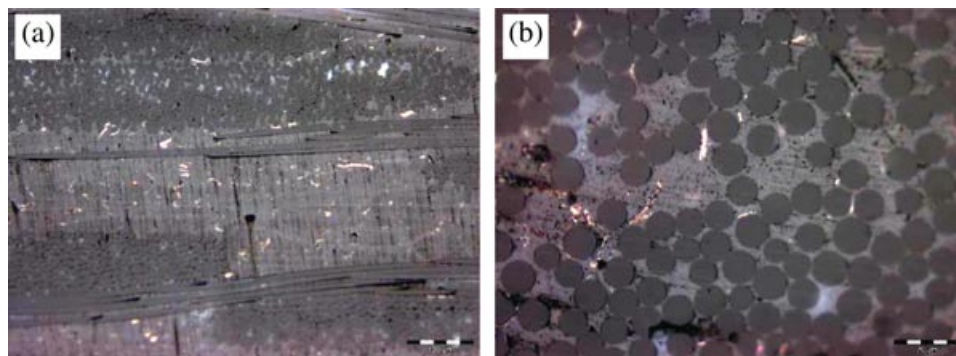
**FIGURE 11.** Optical images of (a) PES+1.0%TG-741 and (b) PES+2.5%TG-741 matrices glass fiber composites.

impregnation defects similar to fractures propagated through the fiber bundles (indicated by arrows in Fig. 10b). These defects are likely to be caused by the high viscosity at low shear rates (nonterminal behavior) of these matrices.

In all the continuous fiber composites, based on graphite-filled PES, the fibers were homogeneously impregnated and large graphite platelets were distributed in the matrix between glass fiber fabric layers (Fig. 11a). Graphite platelets have also penetrated inside the glass fiber bundles and, in some case, located at fibers/matrix interface as illustrated in Fig. 11b. This adaptability of graphite platelets is due to their low out of plane elastic modulus (4.5 GPa).[16,28]

The SEM analysis of glass fibers surfaces from neat matrix composites has indicated a good interfacial adhesion, since after sample fracture a thin polymer layer still coated the glass fiber (Fig. 12a). The fibers surface of the composites based on nanofilled matrix also displayed a polymeric coating layer, but the silica particles agglomerates and graphite platelets were embedded in this layer (Figs. 12b and 12c). The silica agglomerates were round shaped, and their appearance was similar to that of cryogenically fractured matrix evidenced in SEM images (Fig. 5). The graphite platelets, disk-like in shape and similar to the smaller platelets of Fig. 6a, were partially incorporated in PES layers and protruded from the fiber. During the fibers impregnation by the nanofilled matrix in the composite manufacturing process, graphite platelets may be sieved by the glass fibers bundles, allowing only the smallest particles to penetrate between the fibers. The presence of particles (either nanosilica or graphite) at fiber/matrix interfaces did not apparently result in interface properties reduction since most of the mechanical properties of nanofilled matrix composites in the dry state were improved or at least unchanged. On the contrary, mechanical tests on composites dipped in acetone showed some features that could be related to interface properties deterioration.
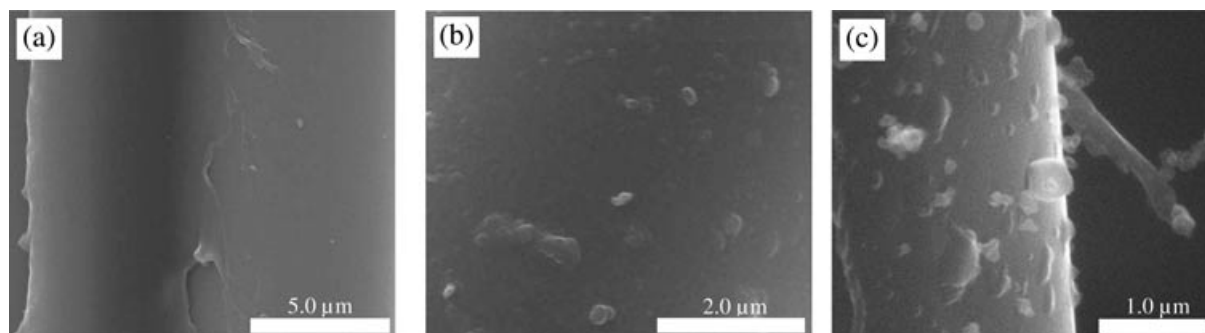


**FIGURE 12.** SEM image of glass fibers from fractured surface upon flexural test. Composites prepared with matrices: (a) neat PES, (b) PES+1.0%R380, and (c) PES+1.0TG-741.

## MECHANICAL TESTS

To take into account the effect of the small variations of glass fibers volume content in composites on mechanical properties, the measured average flexural modulus and strength were corrected by multiplying the measured value by the fiber volume correction factor $0.5/V_f$ (where $V_f$ is the measured volume fraction of the composites).[37] In any case, the deviation from reference fiber volume fraction (0.5) and the corrected values of modulus and strength was smaller than 6% and 10%, respectively.

The flexural modulus of all nanofilled matrix composites increased with respect to the modulus of neat PES matrix composite and PES+1.0%TG-741 matrix composite presented the highest flexural modulus increment (Table IV). The flexural strength of the composites based on nanosilica matrix slightly increased at 0.5% filler concentration; however, it decreased for the PES+2.5%R380 matrix composite. The flexural strength of all the graphite-based matrix composites increased relatively to that of neat PES matrix composite. In particular, the composite prepared with PES+2.5%TG-741 presented the highest flexural strength value (16% higher than neat PES composite flexural strength). The strains at maximum stress measured in flexural tests showed a negligible variation with the filler content of the matrix (Table IV). The results from short-beam shear test have revealed an increase of the shear strength for all samples containing graphite. While the shear strength of nanosilica-based matrix composites was almost unchanged, except for the PES+2.5%R380 matrix composite, whose strength decreased of 10%. The shear strength of PES+1.0%TG-741 matrix composite increased of 26% with respect to the neat PES composite, while the increment of the

other graphite-based matrix composites was higher than 10%.

Although the nanofiller content was very low, a relevant increase in both flexural modulus and strength were measured. These results are even more relevant if one considers that the selected nanofillers displayed neither a high reinforcing efficiency (nanosilica) nor a strong interaction with matrix (expanded graphite). Only PES+2.5%R380 matrix composite exhibited a reduction in both flexural and shear strength, due to impregnation defects, clearly detectable through optical microscopy investigations.

The shear strength enhancement of the PES+1.0%TG-741 matrix composite could be related to the reinforcement effect of graphite particle located between glass fiber fabrics. This could be due to a maximum in the shear properties occurring at 1.0 vol% content. In fact, in short beam shear tests higher properties can be obtained when some fibers are misaligned and oriented out of the plane of the laminate, so that the measured breaking force is partly attributable to the stretching and possible fracture of some fibers.[38] Indeed, graphite platelets could have played an effective reinforcing role in shear strength, since their orientation was not predominantly parallel to the laminate plane (Fig. 11a).

To investigate the mechanical properties decay of continuous fibers composites upon immersion in acetone, flexural tests were performed on composite samples dipped in acetone at 30°C for two time intervals: 1 and 5 days. After 5 days, mechanical properties became very poor for all samples due to acquired rubbery nature of the soaked matrix. Nevertheless, the flexural tests performed after 1 day showed a significant decrease in both

**TABLE IV** ◼

**Mechanical Properties of Continuous Glass Fibers Composites**

| Composite Matrices | Flexural Modulus (Gpa) | Flexural Strength (Mpa) | Strain at Maximum Stress (m/m) | Apparent Shear Strength (Mpa) | Flexural Modulus After 1 Day Immersion in Acetone (GPa) | Flexural Strength After 1 Day Immersion in Acetone [GPa] |
|---|---|---|---|---|---|---|
| Neat PES | $15.353 \pm 0.760$ | $309.2 \pm 13.4$ | $2.08 \pm 0.06$ | $36.75 \pm 1.80$ | $8.385 \pm 0.171$ | $192.7 \pm 8.04$ |
| PES+0.5%R380 | $17.392 \pm 1.313$ | $319.4 \pm 16.4$ | $2.20 \pm 0.18$ | $37.55 \pm 1.42$ | $6.507 \pm 1.564$ | $183.4 \pm 10.39$ |
| PES+1.0%R380 | $17.075 \pm 1.197$ | $308.9 \pm 20.0$ | $2.24 \pm 0.12$ | $37.63 \pm 5.17$ | $6.089 \pm 0.837$ | $152.8 \pm 10.46$ |
| PES+2.5%R380 | $17.232 \pm 1.696$ | $295.9 \pm 42.5$ | $2.23 \pm 0.10$ | $32.75 \pm 4.28$ | // | // |
| PES+0.5%TG741 | $18.020 \pm 1.036$ | $316.1 \pm 21.5$ | $2.07 \pm 0.04$ | $41.37 \pm 1.48$ | $7.983 \pm 1.121$ | $173.2 \pm 6.38$ |
| PES+1.0%TG741 | $18.423 \pm 1.210$ | $318.6 \pm 19.4$ | $1.99 \pm 0.09$ | $46.47 \pm 0,72$ | $8.347 \pm 0.871$ | $187.7 \pm 13.70$ |
| PES+2.5%TG741 | $17.380 \pm 0.652$ | $358.5 \pm 22.6$ | $2.34 \pm 0.18$ | $40.14 \pm 2.62$ | $10.886 \pm 2.424$ | $214.9 \pm 40.46$ |

//: not evaluated.

modulus and strength. The mechanical properties of graphite-based matrix composites were comparable to those of neat PES matrix composite, whereas those of silica-based matrix composites were lower (Table IV). The PES+2.5%TG-741 matrix composite yielded the highest flexural strength and modulus, whereas those of PES+2.5%R380 matrix composite were too low to be measured. The properties of the composites were clearly influenced by both type and content of nanoparticles in the matrix. The low mechanical properties of PES+2.5%R380 matrix composite resulted from both decrease in matrix barrier resistance and imperfect fibers impregnation. As demonstrated by solvent uptake and DMA tests, the barrier properties of graphite-filled PES were higher than those of PES+R380. Such better matrix properties resulted in a reduced decay of mechanical properties than that of the silica-based matrix composites. It is worth noting that the mechanical properties values of the PES composite after 1 day of exposure to acetone were comparable to those of graphite-based matrix composite, even though the diffusion coefficient of the neat PES was smaller than that of nanofilled matrices. This is probably due to the negligible deterioration of fiber/matrix interface by nanoparticles[39] in dry conditions, which becomes more prevalent in wet conditions.[38]

# Conclusions

The work carried out has demonstrated that addition of fumed silica or expanded graphite to PES matrix results in remarkable improvement in barrier properties to solvents. Furthermore, nanofilled PES also shows a decrease in solvent uptake at equilibrium. The model proposed to describe the storage modulus decay of PES samples during solvent absorption can accurately fit the experimental data and can be used to calculate the diffusion coefficient. Both types of nanoparticles were dispersed to the nanoscale level in PES at the lowest concentrations, whereas nanoparticles agglomerates were detected at higher filler concentrations. The different degrees of nanoparticles dispersion, which characterizes the different nanocomposite systems, resulted in a non-monotonic increase in the measured properties (such as storage modulus and diffusivity) with the increasing filler content.

In all glass fiber composites prepared with nanofilled PES matrix, a good impregnation was achieved except for the composites with PES+ 1.0%R380 and PES+2.5%R380 matrices, because of the high viscosity of the matrix. All the nanocomposite-based laminates showed flexural and shear properties improvement, indicating that nanoparticles yield a reinforcing effect together with the barrier properties enhancement. However, the addition of nanoparticles to the matrix of continuous fibers laminate did not result in a significant improvement in composite barrier properties.

# References

1. Engineering and High Performance Plastics. Rapra Market Report by David K Platt Rapra Technology Limited, Shrewsbury, UK, June 2003.
2. Peters, S. T. (Ed). Handbook of Composites; Chapman & Hall, London, 1998.
3. Searle, O. B.; Pfeiffer, R. H. Polym Eng Sci 1985, 25, 474.
4. Saleem, A.; Frormann, L.; Iqbal, A. Polym Compos 2007, 28, 785.
5. Wu, G. M.; Schultz, J. M. Polym Compos 2000, 21, 223.
6. Burnside, S. D.; Giannelis, E. P. Chem Mater 1995, 7, 1597.
7. Yano, K.; Usuki, A.; Okada, A. J Polym Sci A: Polym Chem 1997, 35, 2289.
8. Huang, J. C.; Zhu, Z. K.; Yin, J.; Qian, X. F.; Sun, Y. Y. Polymer 2001, 42, 873.
9. Vlasveld, D. P. N.; Groenewold, J.; Bersee, H. E. N.; Picken, S. J. Polymer 2005, 46, 12567.
10. Jana, S. C.; Jain, S. Polymer 2001, 42, 6897.
11. Mascia, L.; Prezzi, L.; Lavorgna, M. Polym Eng Sci 2005, 45, 1033.
12. Vlasveld, D. P. N.; Groenewold, J.; Bersee, H. E. N.; Mendes, E.; Picken, S. J. Polymer 2005, 46, 6102.
13. Vlasveld, D. P. N.; Daud, W.; Bersee, H. E. N.; Picken, S. J. Composite A, 2007, 38, 730.
14. Jen, M. H. R.; Tseng, Y. C.; Wu, C. H. Compos Sci Technol 2005, 65, 775.
15. Akkapeddi, M. K. Polym Compos 2000, 21(4), 576.
16. Kim, H.; Macosko, C. W. Macromolecules 2008, 41, 3317.
17. Ajayan, P. M.; Schadler, L. S.; Braun, P. V. (Eds.). Nanocomposite Science and Technology; Wiley-VCH: Weinheim, Germany, 2003.
18. Lee, K. M.; Han, C. D. Polymer 2003, 44, 4573.

19. Ash, B. J.; Rogers, D. F.; Wiegand, C. J.; Schadler, L. S.; Siegel, R. W.; Benicewicz, B. C.; Apple, T. Polym Compos 2002, 23, 1014.

20. Park, S. K.; Kim, S. H.; Hwang, J. T. Polym Compos 2009, 30, 309.

21. Rong, M. Z.; Zhang, M. Q.; Pan, S. L.; Lehmann, B.; Friedrich, K. Polym Int 2004, 53, 176.

22. Fornes, T. D.; Paul, D. R. Polymer 2003, 44, 4993.

23. Thostenson, E. T.; Li, C. Y.; Chou, T. W. Compos Sci Technol 2005, 65, 491.

24. Wu, C. L.; Zhang, M. Q.; Rong, M. Z.; Friedrich, K. Compos Sci Technol 2005, 65, 635.

25. Kuo, M. C.; Tsai, C. M.; Huang, J. C.; Chen, M. Mater Chem Phys 2005, 90, 185.

26. Lai, Y. H.; Kuo, M. C.; Huang, J. C.; Chen, M. Mater Sci Eng A 2007, 458, 158.

27. Halpin Affdl, J. C.; Kardos, J. L. Polym Eng Sci 1976, 16, 344.

28. Pierson, Hugh O. (Eds.); Handbook of Carbon, Graphite, Diamond and Fullerene; Noyes: Park Ridge, NJ, 1993.

29. Li, Y.; Zhao, B.; Xie, S.; Zhang, S. Polym Int 2003, 52, 892.

30. Nielsen, L. E. J Macromol Sci, A: Pure Appl Chem 1967, 1, 929.

31. Picard, E.; Vermogen, A.; Gerard, J. F.; Espuche, E. J Membr Sci 2007, 292, 133.

32. Riande, E.; Diaz-Calleja, R.; Prolongo, M. G.; Masegosa, R. M.; Salom, C. Polymer Viscoelasticity; Marcel Dekker: New York, 2000.

33. Browne, M. M.; Forsyth, M.; Goodwin, A. A. Polymer 1997, 38, 1285.

34. Pramanik, M.; Acharya, H.; Srivastava, S. K. Macromol Mater Eng 2004, 289, 562.

35. Cranck, J. The Mathematics of Diffusion; Clarendon Press, Oxford, UK, 1975.

36. Carslaw, H. S.; Jaeger, J. C. Conduction of Heat in Solids; Clarendon Press: Oxford, 1959.

37. Vlasveld, D. P. N.; Bersee, H. E. N.; Picken, S. J. Polymer 2005, 46, 10269.

38. Hodgkinson, J. M. (Ed.). Mechanical Testing of Advanced Fibre Composites; Woodhead: London, 2000.

39. Vlasveld, D. P. N.; Parlevliet, P. P; Bersee, H. E. N.; Picken, S. J. Composites, Part A 2005, 36, 1.